

A Self-Consistent Reduced Model for Dusty Magnetorotationally Unstable Discs

Emmanuel Jacquet,¹ Steven Balbus^{2,3}

¹Laboratoire de Minéralogie et de Cosmochimie du Muséum, Muséum National d'Histoire Naturelle, 57 rue Cuvier, 75005 Paris, France

²Laboratoire de Radioastronomie, École Normale Supérieure, 24 rue Lhomond, 75231 Paris CEDEX 05, France

³Institut universitaire de France, Maison des Universités, 103 blvd. Saint-Michel, 75005 Paris, France

11 June 2021

ABSTRACT

The interaction between settling of dust grains and magnetorotational instability (MRI) turbulence in protoplanetary disks is analyzed. We use a reduced system of coupled ordinary differential equations to represent the interaction between the diffusion of grains and the inhibition of the MRI. The coupled equations are styled on a Landau equation for the turbulence and a Fokker-Planck equation for the diffusion. The turbulence-grain interaction is probably most relevant near the outer edge of the disk's quiescent, or “dead” zone. Settling is most pronounced near the midplane, where a high dust concentration can self-consistently suppress the MRI. Under certain conditions, however, grains can reach high altitudes, a result of some observational interest. Finally, we show that the equilibrium solutions are linearly stable.

Key words: protoplanetary discs – turbulence – (magnetohydrodynamics) MHD – instabilities – diffusion.

1 INTRODUCTION

The presence of small dust grains in protostellar disks is critical to the thermal, dynamical, and chemical behavior of the gas, and is a crucial observational diagnostic. One particularly important feature is that dust tends to stabilize disks against the magnetorotational instability (MRI), and to otherwise complicate our understanding of MHD processes in such systems (Stone et al. 2000; Sano et al. 2000; Salmeron & Wardle 2008; Bai & Goodman 2009). By readily adsorbing free electrons onto their surfaces the grains become charge carriers of very low mobility. In addition, the grains deplete the gas of alkali metal atoms, which are ordinarily a low ionization potential source of electrons. This causes the resistivity of the gas-dust mixture to rise dramatically and essentially suppress MRI-powered turbulence over a wide range of heliocentric distances. Indeed, inclusion of dust grains in resistivity calculations result in greater “dead zones” than predicted by gas-phase chemical networks alone (Sano et al. 2000; Bai & Goodman 2009).

Most studies thus far have assumed that dust grains were well-mixed over the vertical thickness of the disk (Sano et al. 2000; Salmeron & Wardle 2008; Bai & Goodman 2009). This is justified for small grains, which are tightly coupled to the gas. However, as grains grow in size, while still controlling the ionization of the gas, and gas becomes less dense, significant decoupling should occur, particularly at large heliocentric distances. In particular, if the gas is stabilized, the embedded grains will settle toward the disk midplane. At

this stage, depleted of its grains, the ionization rises and the gas may once again be vulnerable to the MRI. However, the ensuing turbulent agitation would *restir* the grains, diffusing them once again upward into the gas (e.g. Carballido et al. 2006). Of course, the grains would then suppress the same instability that allowed them to diffuse through the gaseous envelope. The “cycle of inconsistency” would continue...

How is this behavior ultimately resolved? It is possible to envision a middle ground. In a turbulent medium, the growth of fluctuations is generally set by a balance between linear (magnetic tension forces and resistive dissipation) and nonlinear (cascade) processes. If saturation occurs at low amplitudes where nonlinearity is of secondary importance, the balance may be more simply regulated by a marginal, near zero, linear growth rate. The presence of *some* level of turbulent fluctuations would diffuse dust, and rather than cut-off the instability, such diffusion might regulate its growth. Specifically, the turbulence could stir just enough dust into the gas to ensure marginal growth: an increase in fluctuations raises the effective resistivity (more dust), a decrease in fluctuations increases the effective conductivity (less dust). The question of the existence and stability of such a dynamical equilibrium is the focus of the current paper.

Our chosen method of investigation is to construct and study a reduced system of ordinary differential equations, designed to reproduce certain key features of real disks. Our mathematical problem consists of two coupled, nonlinear

equations, both of which are a common staple of reduced systems. The first is a simple nonlinear Landau equation (Landau & Lifshitz 1959) for the fluctuation amplitude. The second is a Fokker-Planck equation, with both drift and diffusive terms, for the concentration of dust grains. The diffusion coefficient of the Fokker-Planck equation is a function of the fluctuation level, whereas the growth rate of the Landau equation depends on the grain concentration. It is this particular mathematical coupling in our proxy system that makes it interesting for astrophysical applications. We are able to demonstrate the existence of stable solutions for our reduced systems.

This article is organized as follows: In Section 2, we investigate the conditions under which the interaction studied is relevant in the disk. In Section 3, we outline our reduced system and its equilibrium solution. Proof of its stability is deferred to Appendix B. In Section 4, we adopt a specific form for the growth rate for illustrative purposes. In Section 5, we conclude.

2 DUST AND MRI: A REVIEW

In this section, we review the role of dust on the MRI in a schematic way to orient the reader with respect to order-of-magnitude scalings, and to highlight the conditions under which the interaction of dust settling with the MRI may be relevant. There are three primary criteria for this:

- (i) The dust dominates recombination of ions and electrons.
- (ii) Nonideal MHD effects are important, but do not suppress MHD turbulence altogether.
- (iii) A substantial fraction of the dust grains can settle to the midplane.

We shall quantify each of these in the next subsections.

The disk is described in a cylindrical coordinate system, with R the heliocentric distance and z the height above the midplane. Since our calculations are local, we need not specify a global disk model but we shall normalize our results to values of order those of the minimum mass solar nebula (MMSN; Hayashi 1981) near an heliocentric distance of 10 AU. We will assume the disk to be axisymmetric and vertically isothermal, with the gas density given by:

$$\rho = \frac{\Sigma}{\sqrt{2\pi}H} \exp\left(-\frac{z^2}{2H^2}\right), \quad (1)$$

with Σ the surface density, c_s the isothermal sound speed, $H = c_s/\Omega$ is the pressure scale height and Ω the Keplerian angular velocity. $P = \rho c_s^2$ is the corresponding pressure.

2.1 The ionization fraction

Consider a gas composed of neutrals, ions and electrons, and a population of dust grains, of respective number densities n_n , n_i , n_e and n_p , all assumed to be at the same temperature T . The neutrals are predominantly H_2 molecules and the ions are treated as one singly-charged species. The grains are assumed to be identical spheres of radius a and internal density ρ_s ; we also denote by $\rho_p = 4\pi\rho_s a^3 n_p/3$ the dust

mass density and by $\epsilon \equiv \rho_p/\rho$ the dust-to-gas mass ratio¹. We denote by ζ the ionization rate, which in the outer solar system shall be dominated by cosmic rays (Bai & Goodman 2009). The evolution equations for n_e and n_i are:

$$\frac{\partial n_e}{\partial t} = \zeta n_n - \beta_{\text{eff}} n_e n_i - I_e \pi a^2 v_{Te} n_p n_e \quad (2)$$

$$\frac{\partial n_i}{\partial t} = \zeta n_n - \beta_{\text{eff}} n_e n_i - I_i \pi a^2 v_{Ti} n_p n_i, \quad (3)$$

where β_{eff} is the effective gas-phase electron-ion recombination rate, $v_{T_{e,i}} \equiv \sqrt{8k_B T/\pi m_{i,e}}$ is a characteristic thermal speed, and $I_{e,i}$ the (averaged) product of the sticking coefficient and the focusing factor due to electrostatic effects (the \tilde{J} of Draine & Sutin 1987).

In the absence of dust grains, using charge neutrality, the fractional abundance of electrons at equilibrium ionization is (Gammie 1996; Fromang et al. 2002):

$$\begin{aligned} x_e \equiv \frac{n_e}{n_n} &= \sqrt{\frac{\zeta}{\beta_{\text{eff}} n_n}} \\ &= 2 \times 10^{-10} \left(\frac{\zeta}{10^{-17} \text{ s}^{-1}} \frac{10^{-16} \text{ m}^3/\text{s}}{\beta_{\text{eff}}} \frac{10^{-9} \text{ kg/m}^3}{\rho} \right)^{1/2} \end{aligned} \quad (4)$$

Since metal ions have a low recombination rate (see Appendix A), a small fraction of their cosmic abundance is then sufficient for x_e to allow widespread MRI activity (Fromang et al. 2002; Bai & Goodman 2009) *if dust is ignored*. The appreciable depletion ($\gtrsim 10\%$) of chondrites in moderately volatile elements (e.g. alkalis) relative to the total condensable matter (e.g. Scott & Krot 2003) suggests that these elements were not very efficiently removed from the *gas* phase. Their depletion in the gas phase likely did not exceed 1-2 orders of magnitude then (similarly to cold interstellar gas, e.g. Yin 2005), in contrast to the much stronger depletions envisioned in some parameter studies (e.g. Fromang et al. 2002; Ilgner & Nelson 2008; Flaig et al. 2012). Metals *per se* would thus be sufficiently abundant to significantly reduce the extent of the dead zone (Fromang et al. 2002; Bai & Goodman 2009) but this does not hold if dust is taken into account (Sano et al. 2000; Bai & Goodman 2009). Dust thus appears as the main agent acting to suppress the MRI.

If gas-phase recombination can be neglected (which we seek here to quantify), we have, at equilibrium:

$$\begin{aligned} x_e = \frac{4}{3} \frac{\zeta \rho_s a}{I_e \rho_p v_{Te}} &= 3 \times 10^{-13} \frac{1}{I_e} \left(\frac{\zeta}{10^{-17} \text{ s}^{-1}} \right) \left(\frac{\rho_s a}{10^{-2} \text{ kg/m}^2} \right) \\ &\quad \left(\frac{10^{-11} \text{ kg/m}^3}{\rho_p} \right) \left(\frac{100 \text{ K}}{T} \right)^{1/2}. \end{aligned} \quad (5)$$

The normalizing value of $\rho_s a = 10^{-2} \text{ kg/m}^2$ applies to micron-sized grains. The smaller the grains, the larger the area offered for recombination per unit mass, and hence the lower the ionization fraction. Since the equilibrium attainment timescale x_e/ζ is shorter than all other timescales of interest, chemical equilibrium will be assumed throughout.

¹ The grains are considered to be sufficiently large to ignore the effects of their electrical charge on their own dynamics and their direct contribution to the current density (see Wardle 2007) and thence nonideal MHD terms (but see Bai (2011) for the effects PAH-sized grains).

Neglect of electron-ion recombination is warranted if:

$$\begin{aligned}
 \frac{\beta_{\text{eff}} n_i n_e}{\zeta n_n} &= \frac{16 (m_e m_i)^{1/2} \beta_{\text{eff}} \zeta}{9 m_{H_2}^2 I_e I_i P} \left(\frac{\rho_s a}{\epsilon} \right)^2 \\
 &\approx \frac{10^{-4}}{I_e I_i} \left(\frac{\zeta}{10^{-17} \text{ s}^{-1}} \right) \left(\frac{\beta_{\text{eff}}}{10^{-16} \text{ m}^3/\text{s}} \right) \\
 &\quad \left(\frac{\rho_s a}{10^{-2} \text{ kg/m}^2} \frac{10^{-2}}{\epsilon} \right)^2 \left(\frac{10^{-3} \text{ Pa}}{P} \right) \\
 &\ll 1.
 \end{aligned} \tag{6}$$

(Some justification of the normalizing value for β_{eff} is provided in Appendix A, where the molecular ion/metal ion ratio is estimated). Under this condition, the dust may be said to control the ionization fraction as required by criterion (i). Note that our focus on dust properties is strictly justified if its impact on the ionization fraction is not overshadowed by vertical variations of the ionization rate, which is satisfied if e.g. the gas column density is smaller than the stopping grammage of the ionizing radiations ($9.6 \times 10^2 \text{ kg/m}^2$ for cosmic rays according to Umebayashi & Nakano 1981).

2.2 MRI activity

The reduced ionization due to dust enhances nonideal terms in the induction equation, whose importance we now quantify. Various dimensionless numbers have been defined in the literature depending on the diffusivity regime, and the thresholds for MRI activation are still being debated, so we shall restrict ourselves to two of them, pertaining to ohmic and ambipolar diffusion, respectively:

Ohmic diffusion is believed to dominate near the midplane (e.g. Salmeron & Wardle 2008). The importance of Ohmic diffusivity η_0 is measured by the magnetic Reynolds number, which, if we inject equation (5), is given by²

$$\begin{aligned}
 \text{Re}_M &\equiv \frac{c_s^2}{\eta_0 \Omega} = \frac{\pi \mu_0 e^2 \sigma_0 \zeta \rho_s a}{8 m_{H_2} I_e \Omega \rho_p} \\
 &= \frac{50}{I_e} \left(\frac{R}{10 \text{ AU}} \right)^{3/2} \left(\frac{\zeta}{10^{-17} \text{ s}^{-1}} \right) \left(\frac{\rho_s a}{10^{-2} \text{ kg/m}^2} \right) \\
 &\quad \left(\frac{10^{-11} \text{ kg/m}^3}{\rho_p} \right).
 \end{aligned} \tag{7}$$

with $\sigma_0 = 10^{-19} \text{ m}^2$ the neutral-electron cross-section (Draine et al. 1983). Currently estimated thresholds for Re_M for good coupling between the gas and magnetic fields are $10^{2\pm 2}$ (Fromang et al. 2002).

The importance of ambipolar diffusion, which may dominate in the upper layers of the disk (Perez-Becker & Chiang 2011), is measured by the dimensionless ion-neutral collision rate (per neutral molecule):

$$\begin{aligned}
 \text{Am} &\equiv \frac{x_i n_n \beta_{\text{in}}}{\Omega} = \frac{4 \beta_{\text{in}} \zeta}{3 I_i m_{H_2} v_{T_i} \Omega} \frac{\rho_s a}{\epsilon} \\
 &= \frac{0.5}{I_i} \sqrt{\frac{m_i}{m_{H_2}}} \left(\frac{\zeta}{10^{-17} \text{ s}^{-1}} \right) \left(\frac{\rho_s a}{10^{-2} \text{ kg/m}^2} \right) \\
 &\quad \left(\frac{10^{-2}}{\epsilon} \right) \left(\frac{100 \text{ K}}{T} \right)^{1/2} \left(\frac{R}{10 \text{ AU}} \right)^{3/2},
 \end{aligned} \tag{8}$$

² We use $\eta_0 = 4v_{T_e} m_e \sigma_0 / (3\mu_0 e^2 x_e)$ from equations (9), (24) and (25) of Balbus (2011).

with $\beta_{\text{in}} = 1.9 \times 10^{-15} \text{ m}^3/\text{s}$ the ion-neutral collision rate coefficient (Draine et al. 1983). The threshold for good coupling between ions and neutrals is of order $1 - 10^2$ (Perez-Becker & Chiang 2011; Bai & Stone 2011).

As mentioned previously, other dimensionless numbers exist in the literature but as these are proportional to the ionization fraction, their dependence on dust properties is subsumed in the factor $\rho_s a / \rho_p$, or equivalently $\rho_s a / \epsilon$.

The condition (ii) that the turbulence level is a strong function of ionization is met when the magnetic coupling is marginally good, i.e. when the dimensionless number pertaining to the relevant diffusivity regime is close to its threshold value for ideal MHD. In other words, the region most relevant to our analysis is near the outer edge of the dead zone. From equations (7) and (8), this edge may be expected to be at $\sim 10 \text{ AU}$ from the Sun in a MMSN, as it was in the detailed calculations of Bai & Goodman (2009).

2.3 Grain dynamics

The dynamics of solid grains are dictated by gas drag. For grains small compared to the gas mean free path, the stopping time is (Epstein 1924)

$$\tau = \sqrt{\frac{\pi}{8}} \frac{\rho_s a}{\rho c_s}. \tag{9}$$

For small grains ($\tau \ll \Omega^{-1}$), the vertical drift velocity of the grains is given by (Dubrulle et al. 1995):

$$v(z) = -\Omega^2 \tau z. \tag{10}$$

Settling is counteracted by turbulent diffusion, which tends to stir dust particles above the midplane. The vertical diffusion coefficient may be parameterized as:

$$D_z = \delta_z \frac{c_s^2}{\Omega}, \tag{11}$$

where δ_z is a dimensionless parameter of order the standard α parameter (e.g. Johansen et al. 2006).

With these notations, equilibrium between diffusion and settling is attained on a timescale

$$t_{\text{vert}} = \frac{1}{\Omega \delta_z \max(1, S_z)} = 50 \text{ ka} \left(\frac{10^{-4}}{\delta_z \max(1, S_z)} \right) \left(\frac{R}{10 \text{ AU}} \right)^{3/2} \tag{12}$$

and the equilibrium thickness of the dust layer is $H_p = H / \sqrt{1 + S_z}$ (Cuzzi et al. 1996). We have introduced

$$\begin{aligned}
 S_z &\equiv \frac{\Omega \tau}{\delta_z} = \frac{\pi \rho_s a}{2 \Sigma \delta_z} \\
 &= 20 \left(\frac{\rho_s a}{10^{-2} \text{ kg/m}^2} \right) \left(\frac{10^{-5}}{\delta_z} \right) \left(\frac{10^2 \text{ kg/m}^2}{\Sigma} \right),
 \end{aligned} \tag{13}$$

where τ and δ_z are evaluated at the midplane ($z = 0$). S_z is thus a measure of the settling of dust relative to the gas. Significant settling of dust, with interesting feedback on the MRI, corresponds to $S_z \gg 1$. This implies (1) relatively low surface densities (as expected far from the Sun) (2) relatively big grains, say $10^{1\pm 1} \mu\text{m}$ (but likely no larger for dust to retain control of the ionization fraction), presumably as a result of coagulation or (3) a low turbulence level around the midplane, or a combination thereof. Low values of $\delta_z < 10^{-4}$ are seen around the midplane in numerical simulations of layered accretion (e.g. Fleming & Stone 2003;

Igner & Nelson 2008; Oishi & Mac Low 2009; Turner et al. 2010; Okuzumi & Hirose 2011; Flaig et al. 2012). Note that while Turner et al. (2010) did account self-consistently for the dynamics of dust as well as its role on the ionization fraction, no significant effect of dust motion was found (see e.g. their figure 14), but this is because maximum (midplane) values of S_z were only 0.2, 0.8 and 1 for the runs with 1 μm , 10 μm and 100 μm grains, respectively³.

With these numerical estimates setting the scales, we turn to a reduced model of interaction between dust and MRI turbulence.

3 REDUCED MODEL

3.1 General Equations

Consider a vertical section of a protostellar disk. We denote by y a turbulent fluctuation of the gas (with ϵ still denoting the dust-to-gas ratio). Our reduced model consists of the following system of equations:

$$\rho \frac{\partial \epsilon}{\partial t} = \frac{\partial}{\partial z} \left[\rho \left(Qy^2 \frac{\partial \epsilon}{\partial z} - v(z)\epsilon \right) \right] \quad (14)$$

$$\frac{\partial y}{\partial t} = \gamma(\epsilon)y - Ay^3 \quad (15)$$

Equation (15) may also be rewritten as:

$$\frac{\partial y^2}{\partial t} = 2\gamma(\epsilon)y^2 - 2Ay^4 \quad (16)$$

The first equation (14) is a diffusion equation for the grains with a drift term proportional to the velocity $v(z)$. It has a standard Fokker-Planck form. The second equation (15) is a Landau equation (Landau & Lifshitz 1959) for nonlinearly damped fluctuations. The constant Q relates y to the vertical diffusion coefficient $D_z = Qy^2$ and the constant A characterizes the nonlinear saturation. Linear growth and damping (here MRI-driven) are embodied in γ the nominal rate coefficient, which depends on ϵ by assumptions (i) and (ii) in Section 2. The form of $\gamma(\epsilon)$ is at this point unprescribed, but it is assumed to be a positive, differentiable quantity. Physically, we would expect it to be a monotonically decreasing function of ϵ . It would reach an asymptotic value for ϵ below the threshold for recombination on dust grains to be important (see equation (6)), which corresponds to the dust-free (not necessarily ideal) MHD turbulence value. For ϵ above another threshold, MRI-powered turbulence is suppressed, but other instabilities (e.g. Weidenschilling 1980; Youdin & Goodman 2005; Latter et al. 2010; Lesur & Papaloizou 2010) may help maintain a minimum level of turbulence and establish a dynamical equilibrium.⁴

³ We identify δ_z with α evaluated from their figure 7.

⁴ The Landau equation used here ignores any transport within the gas, e.g. from the active layers to the dead zone (Fleming & Stone 2003; Turner & Sano 2008) but were we to add a term $\frac{\partial}{\partial z} \left(Qy^2 \frac{\partial y^2}{\partial z} \right)$ in the Landau equation (16), its ratio with e.g. Ay^4 would be of order $Qk^2/A \sim (\Omega/\gamma)(S_z + 1)\delta_z \ll 1$ with $k \sim H_p^{-1}$ the reciprocal lengthscale of variation and it would thus be negligible.

3.2 Equilibrium solution

Equilibrium implies:

$$\frac{\partial \ln \epsilon}{\partial z} = \frac{v(z)}{Qy^2} \quad (17)$$

$$y^2 = \frac{\gamma(\epsilon)}{A} \quad (18)$$

Plugging equation (18) in equation (17) and integrating with respect to z yields:

$$\int_{\epsilon(0)}^{\epsilon} \frac{\gamma(\epsilon)}{\gamma_{df}} \frac{d\epsilon}{\epsilon} = -S_{zdf} \left(e^{z^2/2H^2} - 1 \right), \quad (19)$$

where we have introduced $\gamma_{df} \equiv \gamma(\epsilon = 0)$, the dust-free value of the growth rate, and $S_{zdf} = A\tau(0)c_s^2/\gamma_{df}$ the corresponding value of S_z . The value of $\epsilon(0)$ must satisfy:

$$\bar{\epsilon} \equiv \frac{1}{\Sigma} \int_{-\infty}^{+\infty} \rho_p(z) dz = \frac{1}{\sqrt{2\pi}H} \int_{-\infty}^{+\infty} \epsilon(z) e^{-z^2/2H^2} dz, \quad (20)$$

where we have introduced the dust-to-gas column density ratio $\bar{\epsilon}$. If we approximate $\epsilon(0) \approx \bar{\epsilon}\sqrt{1 + S_z}$ (see Section 2.3), where S_z is evaluated at the midplane, this may be replaced by the following simplified relation:

$$S_z = S_{zdf} \frac{\gamma_{df}}{\gamma(\bar{\epsilon}\sqrt{1 + S_z})}. \quad (21)$$

In principle, depending on the mathematical expression of $\gamma(\epsilon)$ and on the values of S_{zdf} and $\bar{\epsilon}$, it is conceivable that more than one solution exists in terms of S_z , or, equivalently, $\epsilon(0)$, or even none if γ vanishes too rapidly with increasing ϵ (which however seems unrealistic, see Section 3.1).

We show in Appendix B that *regardless* of the form of $\gamma(\epsilon)$, the equilibrium is linearly *stable*. From equation (B6) in the appendix, one estimate the damping timescale to be $t_{\text{vert}}(\lambda/H_p)^2$ with λ the vertical lengthscale of variation of the perturbation: this is basically a diffusion timescale. Physically, if we schematically distinguish between a “midplane zone” and an “atmosphere zone”, we may interpret the lack of instability due to a dust-controlled diffusivity as follows: if the “atmosphere” has excess dust, diminishing turbulence there will make the dust flow toward the midplane to cancel the corresponding dust depletion. If, on the other hand, the atmosphere has a dust depletion, enhanced turbulence will soak the excess dust from the midplane through the “interface” between the two.

4 EXAMPLE

As an example, consider the following functional dependence for the growth rate:

$$\gamma(\epsilon) = \frac{\gamma_{df}}{1 + \epsilon/\epsilon_*}. \quad (22)$$

One may think of ϵ_* as the critical value of ϵ for which the relevant dimensionless number of Section 2.2 is at its threshold value. The asymptotic value of the growth rate for $\epsilon \gg \epsilon_*$ is zero, i.e. we ignore any “background” hydrodynamical turbulence.

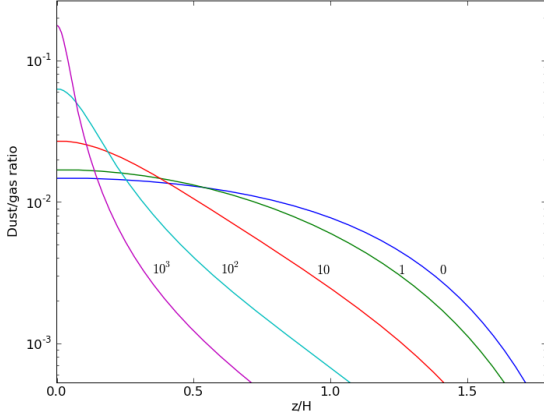


Figure 1. Plot of the equilibrium dust-to-gas ratio ϵ profile, assuming the dependence of the growth rate on ϵ in equation (22). Curves are drawn for $S_{zdf} = 1$ (i.e., marginal settling for dust-free turbulence levels) for different values of $\epsilon(0)/\epsilon_*$ as marked on the figure, assuming a dust/gas column density ratio of 10^{-2} .

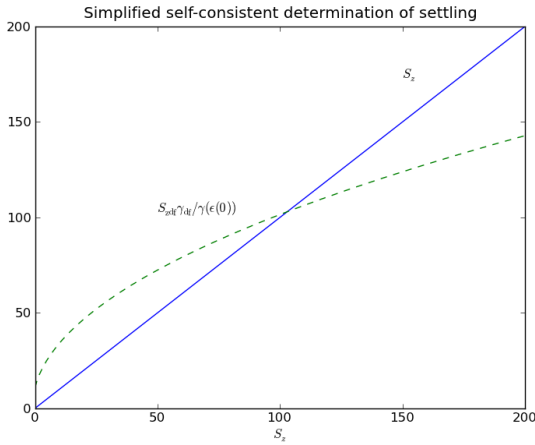


Figure 2. Plot of the left-hand-side (continuous) and the right-hand-side (dashed) of the simplified equation (21) for the example functional dependence of the growth rate displayed in equation (22). For any parameter, there is always one unique solution (corresponding to the intersection between the two curves) for this functional dependence. Here, $\bar{\epsilon}/\epsilon_* = 10$ and $S_{zdf} = 1$.

We obtain from equation (19):

$$\epsilon(z) = \left(\left(\frac{1}{\epsilon_*} + \frac{1}{\epsilon(0)} \right) \exp \left(S_{zdf} (e^{z^2/2H^2} - 1) \right) - \frac{1}{\epsilon_*} \right)^{-1}. \quad (23)$$

This is plotted in Fig. 1. It is seen that enhanced dust abundance at the midplane entails an enhanced settling efficiency, hence a peaked distribution. But as $|z|$ increases and thus the dust fraction drops, turbulence can increase and the profile becomes shallower, until dust no longer affects the turbulence level, by which altitude one has:

$$\epsilon(z) \approx \frac{\exp(-S_{zdf}(e^{z^2/2H^2} - 1))}{\frac{1}{\epsilon_*} + \frac{1}{\epsilon(0)}}, \quad (24)$$

that is, $(1 + \epsilon(0)/\epsilon_*)^{-1}$ times the result for a vertically con-

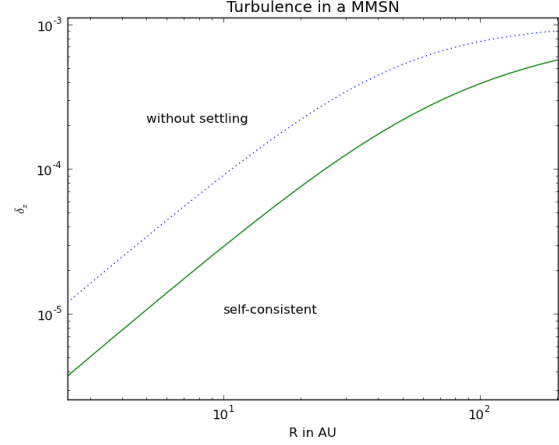


Figure 3. Radial variation of the turbulence parameter δ_z (evaluated at the midplane) in a MMSN assuming that the growth rate is given by equation (22). We assume a constant dust-to-gas column density ratio $\bar{\epsilon} = 0.01$, $\rho_s a = 0.1 \text{ kg/m}^2$ (i.e. $30 \mu\text{m}$ -radius grains), $\delta_{zdf} = 10^{-3}$ and take $\epsilon_* = 10^{-3}(R/10 \text{ AU})^3/2$ (to mimic the dependence on Ω of dimensionless numbers pertaining to nonideal MHD in Section 2.2). The dotted line is the estimate ignoring vertical settling and the continuous line is the self-consistent estimate using simplified equation (21).

stant δ_z (e.g. Fromang & Nelson 2009), a depletion due to the aforementioned enhanced dust concentration at the midplane. If $\epsilon(0) \gg \epsilon_*$, the self-consistently determined dust concentration profile sets the vertical extent of the dead zone and the active layers.

The mass balance constraint on dust expressed by equation (20) reads here:

$$\bar{\epsilon} = \frac{2}{\sqrt{\pi}} \int_0^{+\infty} \frac{e^{-x^2}}{\left(\frac{1}{\epsilon_*} + \frac{1}{\epsilon(0)} \right) \exp(S_{zdf}(e^{x^2} - 1)) - \frac{1}{\epsilon_*}} dx \quad (25)$$

Since the right-hand-side is a monotonic function of $\epsilon(0)$, increasing from 0 to $+\infty$, there is always one unique solution, given S_{zdf} and $\bar{\epsilon}$.

The simplified equation (21), illustrated graphically in Fig. 2, may be solved for S_z as:

$$S_z = S_{zdf} \left[1 + \frac{S_{zdf}}{2} \left(\frac{\bar{\epsilon}}{\epsilon_*} \right)^2 + \sqrt{\left(1 + S_{zdf} \right) \left(\frac{\bar{\epsilon}}{\epsilon_*} \right)^2 + \frac{S_{zdf}^2}{4} \left(\frac{\bar{\epsilon}}{\epsilon_*} \right)^4} \right] \quad (26)$$

If $\bar{\epsilon} \ll \epsilon_*$ and $S_{zdf}(\bar{\epsilon}/\epsilon_*)^2 \ll 1$, there is essentially no effect of dust and $S_z \approx S_{zdf}$. At the other extreme, if $S_{zdf} \max((\bar{\epsilon}/\epsilon_*), (\bar{\epsilon}/\epsilon_*)^2) \gg 1$, we have:

$$S_{zdf} \approx \left(S_{zdf} \frac{\bar{\epsilon}}{\epsilon_*} \right)^2 = \left(\frac{\pi}{2} \frac{\bar{\epsilon}}{\Sigma \delta_{zdf} c_*} \right)^2, \quad (27)$$

where we have set $\epsilon_* = c_* \rho_s a$, with c_* independent of dust properties, in order to account for the dependence of the ionization fraction on grain size (see Section 2.1). We see that, in this limit, the dependences of settling on grain size cancel out. This is because for a given dust concentration, larger grains drift more rapidly toward the midplane, but at

the same time allow higher turbulence levels. Certainly, this (asymptotically) exact cancellation is specific to the dependence we have chosen, but the simulations of Turner et al. (2010) show only a weak dependence of S_z on size, with the former varying by a factor of ~ 5 despite a two-order-of-magnitude variation of the latter (see Section 2.3).

Extrapolating for a range of heliocentric distances, we have plotted the radial profile of δ_z *evaluated at the mid-plane* in figure 3. It is seen that ignoring settling of grains leads to an overestimate of δ_z and hence an underestimate of the heliocentric distance of the outer edge of the dead zone. This is because settling induces larger dust concentrations at the midplane, compared to the perfect vertical mixing assumption, and thus lower turbulence levels there. As to the *vertically averaged* δ_z —a proxy for the standard α parameter—ignoring settling would lead to an underestimate of its value, since γ is here a convex function of ϵ , but in general, the effect of settling on this average depends on the particular mathematical form of $\gamma(\epsilon)$.

5 CONCLUSION

We have studied the interaction between MRI turbulence and dust grains, allowing the dust to control the ionization level (and thus MHD turbulence level), while turbulent fluctuations inhibit dust grain settling to the disk midplane. We have used a reduced model consisting of two coupled equations: a Landau equation for the turbulent fluctuation amplitude and a Fokker-Planck equation governing the vertical dynamics of the grains via a fluctuation-dependent diffusion coefficient. Unconditionally stable equilibrium solutions for the vertical grain distribution were found. Compared with models in which the turbulent fluctuation level is constant with height, the solutions were significantly more concentrated near the midplane, with a lower level of MHD turbulence in this region.

From simple estimates of the ionization fraction and the settling parameter, we found that the interaction studied here is most relevant near the outer edge of the disk's dead zone. Indeed, the grains are likely to determine the dead zone morphology, and will likely control the region's heliocentric extent. Also, an enhanced settling could lead to flatter disks and hence steeper decreases of temperature with heliocentric distance. Thus, the model may be used in conjunction with numerical simulations (global or local), to sharpen observational predictions that will be of great interest when ALMA becomes fully operational.

ACKNOWLEDGMENTS

We thank the anonymous referee for his/her review and for bringing some additional caveats to our model.

REFERENCES

- Bai, X. & Goodman, J. 2009, *ApJ*, 701, 737
 Bai, X.-N. 2011, *ApJ*, 739, 51
 Bai, X.-N. & Stone, J. M. 2011, *ApJ*, 736, 144
 Balbus, S. A. 2011, *Magnetohydrodynamics of Protostellar Disks*, ed. P. J. V. Garcia (University of Chicago Press), 237–282
 Carballido, A., Fromang, S., & Papaloizou, J. 2006, *Monthly Notices of the Royal Astronomical Society*, 373, 1633
 Cuzzi, J. N., Dobrovolskis, A. R., & Hogan, R. C. 1996, in *Chondrules and the Protoplanetary Disk*, ed. R. Hewins, R. Jones, & E. Scott, 35–43
 Draine, B. T., Roberge, W. G., & Dalgarno, A. 1983, *ApJ*, 264, 485
 Draine, B. T. & Sutin, B. 1987, *ApJ*, 320, 803
 Dubrulle, B., Morfill, G., & Sterzik, M. 1995, *Icarus*, 114, 237
 Epstein, P. S. 1924, *Phys. Rev.*, 23, 710
 Flaig, M., Ruoff, P., Kley, W., & Kissmann, R. 2012, *MNRAS*, 420, 2419
 Fleming, T. & Stone, J. M. 2003, *ApJ*, 585, 908
 Fromang, S. & Nelson, R. P. 2009, *A&A*, 496, 597
 Fromang, S., Terquem, C., & Balbus, S. A. 2002, *MNRAS*, 329, 18
 Gammie, C. F. 1996, *ApJ*, 457, 355
 Hayashi, C. 1981, *Progress of Theoretical Physics Supplement*, 70, 35
 Ilgner, M. & Nelson, R. P. 2008, *Astronomy & Astrophysics*, 483, 815
 Johansen, A., Klahr, H., & Mee, A. J. 2006, *MNRAS*, 370, L71
 Landau, L. D. & Lifshitz, E. M. 1959, *Fluid mechanics*, ed. Landau, L. D. & Lifshitz, E. M.
 Latter, H. N., Bonart, J. F., & Balbus, S. A. 2010, *MNRAS*, 405, 1831
 Lesur, G. & Papaloizou, J. C. B. 2010, *A&A*, 513, A60
 Lodders, K. 2003, *ApJ*, 591, 1220
 Oishi, J. S. & Mac Low, M.-M. 2009, *ApJ*, 704, 1239
 Okuzumi, S. & Hirose, S. 2011, *The Astrophysical Journal*, 742, 65
 Perez-Becker, D. & Chiang, E. 2011, *ApJ*, 727, 2
 Salmeron, R. & Wardle, M. 2008, *MNRAS*, 388, 1223
 Sano, T., Miyama, S. M., Umebayashi, T., & Nakano, T. 2000, *ApJ*, 543, 486
 Scott, E. R. D. & Krot, A. N. 2003, *Treatise on Geochemistry*, 1, 143
 Stone, J. M., Gammie, C. F., Balbus, S. A., & Hawley, J. F. 2000, *Protostars and Planets IV*, 589
 Turner, N. J., Carballido, A., & Sano, T. 2010, *ApJ*, 708, 188
 Turner, N. J. & Sano, T. 2008, *ApJ Letters*, 679, L131
 Umebayashi, T. & Nakano, T. 1981, *PASJ*, 33, 617
 Wardle, M. 2007, *Astrophysics and Space Science*, 311, 35
 Weidenschilling, S. J. 1980, *Icarus*, 44, 172
 Yin, Q. 2005, in *Astronomical Society of the Pacific Conference Series*, Vol. 341, *Chondrites and the Protoplanetary Disk*, ed. A. N. Krot, E. R. D. Scott, & B. Reipurth, 632–644
 Youdin, A. N. & Goodman, J. 2005, *ApJ*, 620, 459

APPENDIX A: ESTIMATION OF THE MOLECULE/METAL ION RATIO

In this appendix, we provide some justification of the normalization chosen for β_{eff} in Section 2.1. To that end, we estimate the ratio between the number density n_{m^+} of molecular ions (m^+ , e.g. HCO^+) and that n_{M^+} of metal ions (M^+ , e.g. Mg^+ , Na^+). We thus need to refine the model in the main text by distinguishing between the two. The resulting governing equations are the same as Fromang et al. (2002), whose notation we adopt, with the addition of grains:

$$\frac{\partial n_{m^+}}{\partial t} = \zeta n_n - \beta n_e n_{m^+} - \beta_i n_M n_{m^+} - I_{m^+} \pi a^2 v_{TM^+} n_p n_{m^+} \quad (\text{A1})$$

$$\frac{\partial n_{M^+}}{\partial t} = \beta_i n_M n_{m^+} - \beta_r n_{M^+} n_e - I_{M^+} \pi a^2 v_{TM^+} n_p n_{M^+}, \quad (\text{A2})$$

with n_M the metal number density, $\beta = 3 \times 10^{-13}$ ($100 \text{ K}/T$)^{1/2} m³/s the dissociative recombination rate coefficient for molecular ions, $\beta_r = 3 \times 10^{-18}$ ($100 \text{ K}/T$)^{1/2} m³/s the radiative recombination rate coefficient for metal atoms and $\beta_i = 3 \times 10^{-15}$ m³/s the rate coefficient of charge transfer from molecular ions to metal atoms.

Equation (3) is retrieved by summing these equations, recalling that $n_i = n_{m^+} + n_{M^+}$, if one puts:

$$\frac{1}{\sqrt{m_i}} = \frac{1}{n_i} \left(n_{M^+} \frac{1}{\sqrt{m_{M^+}}} + n_{m^+} \frac{1}{\sqrt{m_{m^+}}} \right) \quad (\text{A3})$$

$$I_i = \sqrt{m_i} \left(\frac{I_{M^+}}{\sqrt{m_{M^+}}} \frac{n_{M^+}}{n_i} + \frac{I_{m^+}}{\sqrt{m_{m^+}}} \frac{n_{m^+}}{n_i} \right) \quad (\text{A4})$$

$$\beta_{\text{eff}} = \frac{n_{M^+}}{n_i} \beta_r + \frac{n_{m^+}}{n_i} \beta \quad (\text{A5})$$

At equilibrium, provided that

$$\frac{\beta_r n_{M^+} n_e}{I_{M^+} v_{TM^+} \pi a^2 n_p n_{M^+}} = \frac{4}{3} \frac{x_e \beta_r \rho_s a}{\epsilon I_{M^+} v_{TM^+} m_{H_2}} \ll 1, \quad (\text{A6})$$

that is, if we plug in equation (5) for x_e ,

$$\left(\frac{\rho_s a}{\epsilon} \right)^2 \frac{\sqrt{m_e m_{M^+}}}{I_e I_{M^+} m_{H_2}^2} \frac{\zeta \beta_r}{P} \ll 1, \quad (\text{A7})$$

which, given that $\beta_r \ll \beta$, is essentially guaranteed by inequality (6), we draw from equation (A2):

$$\frac{n_{m^+}}{n_{M^+}} = \frac{3}{4} \frac{I_{M^+} v_{TM^+} m_{H_2} \epsilon}{\rho_s a \beta_i x_M} = 10^{-3} I_{M^+} \left(\frac{T}{100 \text{ K}} \right)^{1/2} \left(\frac{\epsilon}{10^{-2}} \right) \left(\frac{10^{-2} \text{ kg/m}^2}{\rho_s a} \right) \left(\frac{10^{-7}}{x_M} \right) \quad (\text{A8})$$

where $x_M \equiv n_M/n_n$. It is normalized to a reasonable value considering the solar abundances for e.g. Na, Mg, Si, K, Fe ($\log(M/H) = -5.70, -4.45, -4.46, -6.89, -4.53$, respectively; Lodders 2003) and the expected 1-2 order-of-magnitude depletion due to condensation (see Section 2.1). Then, to a good approximation (if that ratio is larger than 10^{-5}), $\beta_{\text{eff}} \approx (n_{m^+}/n_{M^+})\beta$, justifying the normalization

chosen for β_{eff} in inequality (6). The latter then becomes:

$$\begin{aligned} \frac{\beta_{\text{eff}} n_i n_e}{\zeta n_n} &\approx \frac{\sqrt{m_e m_i}}{m_{H_2}} \frac{I_{M^+}}{I_e I_i} \frac{\beta}{\beta_i} \frac{v_{TM^+}}{x_M} \frac{\rho_s a}{\epsilon} \frac{\zeta}{P} \\ &\approx 10^{-4} \left(\frac{\zeta}{10^{-17} \text{ s}^{-1}} \right) \left(\frac{10^{-3} \text{ Pa}}{P} \right) \left(\frac{10^{-2}}{\epsilon} \right) \\ &\quad \left(\frac{\rho_s a}{10^{-2} \text{ kg/m}^2} \right) \left(\frac{10^{-7}}{x_M} \right) \\ &\ll 1 \end{aligned} \quad (\text{A9})$$

APPENDIX B: LINEAR STABILITY ANALYSIS

We consider the behavior of the equilibrium solution of our reduced model system (14) and (16) to linear perturbations with a time dependence of the form $\exp(st)$. The linearized form of equations (14) and (16) is:

$$s\rho\delta\epsilon = \frac{\partial}{\partial z} \left(\rho \left(Qy^2 \frac{\partial\delta\epsilon}{\partial z} + Q \frac{\partial\epsilon}{\partial z} \delta y^2 - v(z)\delta\epsilon \right) \right) \quad (\text{B1})$$

$$s\delta y^2 = 2\gamma'(\epsilon)y^2\delta\epsilon + 2(\gamma(\epsilon) - 2Ay^2)\delta y^2. \quad (\text{B2})$$

Using background equation (18), equation (B2) yields:

$$\delta y^2 = \frac{\gamma'(\epsilon)y^2\delta\epsilon}{\gamma(\epsilon) + s/2}, \quad (\text{B3})$$

Then, using equation (17), and provided $2\gamma + s \neq 0$, equation (B1) may be rewritten as:

$$s\rho\delta\epsilon = \frac{\partial}{\partial z} \left(\rho \frac{Qy^2}{h} \frac{\partial}{\partial z} (h\delta\epsilon) \right) \quad (\text{B4})$$

With⁵:

$$h = \begin{cases} \frac{1}{\epsilon} |\gamma + \frac{s}{2}| & \text{if } \text{Im}s = 0 \\ \frac{1}{\epsilon} |\gamma + \frac{s}{2}| \exp(-i \arctan \frac{2\gamma + \text{Res}s}{\text{Im}s}) & \text{if } \text{Im}s \neq 0 \end{cases} \quad (\text{B5})$$

where Re and Im denote the real and imaginary parts, respectively. If we multiply equation (B4) by $(h\delta\epsilon)^*$ and integrate over z , we obtain:

$$s = - \frac{\int_{-\infty}^{+\infty} \frac{Qy^2}{h} \left| \frac{\partial}{\partial z} (h\delta\epsilon) \right|^2 \rho dz}{\int_{-\infty}^{+\infty} h^* |\delta\epsilon|^2 \rho dz} \quad (\text{B6})$$

We now want to show that this equation implies that the real part of s (i.e. the growth rate of the perturbation) is negative, i.e. that the system is linearly stable. We distinguish two cases:

Case 1: $\text{Im}s = 0$. In this case h is real and positive. It is then clear from equation (B6) that s must be real and negative⁶.

Case 2: $\text{Im}s \neq 0$. We proceed *ab absurdo*, by supposing $\text{Res} > 0$. Then, $2\gamma + \text{Res}$ is always strictly positive, from

⁵ We use the fact that

$$\frac{d}{dt} \left(\ln|t-w| + i \arctan \frac{t - \text{Re}w}{\text{Im}w} \right) = \frac{1}{t-w},$$

for t a real variable and w a complex constant.

⁶ Recall that in writing equation (B6), we had assumed that $2\gamma + s$ was nonzero everywhere; if that is not the case, it is clear that s would be a negative real number in that case too.

which it follows, from the definition of h (equation (B5)) that:

$$\begin{cases} -\frac{\pi}{2} < \operatorname{arg}h < 0 & \text{if } \operatorname{Im}s > 0 \\ 0 < \operatorname{arg}h < \frac{\pi}{2} & \text{if } \operatorname{Im}s < 0 \end{cases} \quad (\text{B7})$$

where $\operatorname{arg}h$ is the real number (between $-\pi$ and π) satisfying $h = |h|\exp(i\operatorname{arg}h)$. In the complex plane, for a given eigenvector (and thus a fixed $\operatorname{Im}s$), h is thus confined to a determined quadrant. Thus, the integrand in each of the integrals of (B6) is always in the symmetric quadrant with respect to the real axis (because $\operatorname{arg}(1/h) = \operatorname{arg}(h^*) = -\operatorname{arg}h$). Same holds for the integrals themselves. It follows that the *phase* of the *ratio* of these two integrals, which equals the *difference* of the *phases* of these two integrals, cannot be larger than $\pi/2$ in absolute value. In other words, the ratio of the integrals has a positive real part and hence $\operatorname{Re}s < 0$. This contradicts the hypothesis and s must thus have a negative real part.